E. 研究発表

1. 論文発表

　　　無し

2. 学会発表

　　　無し

F. 知的財産権の出願・登録状況

　　　無し

厚生労働科学研究費補助金（医療技術実用化総合研究事業）

総括研究報告書

急性心筋梗塞治療薬に対する新規治療薬の開発

（H25-医療技術-一般-002）

分担研究者　　清水　佳隆　　株式会社バイオメッドコア

研究要旨　急性心筋梗塞発症数は過去 20 年間に 2 倍に増加している。繰り返して入院加療が必要な　梗塞後心不全患者が増加しており、国民医療費増大の一因となっている。そのため、梗塞後心不全進展を抑制する治療法の開発は重要なアンメットニーズである。心筋梗塞による細胞死はミトコンドリア Permeability Transition Pore （mPTP）が開口し，チトクロム C の遊離により誘導される。動物実験・探索的臨床試験において、mPTP 開口阻害薬であるサイクロスポリンA（CsA）による心筋梗塞サイズ縮小効果が報告されたが、CsA は免疫抑制などの副作用を誘発するため、その臨床投与量に制限がある。申請者は代表研究者として、厚生労働科研医療機器開発推進研究事業＜ナノサイズリポソームを用いた急性心筋梗塞治療法の開発＞で、ナノサイズリポソームが障害心筋へ特異的に集積し、リポソームに封入された心保護薬の薬効増強と副作用軽減を世界に先駆けて見出した。本技術を用い、既に、ラット心筋梗塞モデルにおいて、低用量リポソーム化 CsA（Lipo-CsA）による心筋梗塞サイズ縮小増強効果を確認した。さらに、平成 25 年度末までに、薬効薬理試験、薬物動態試験、製剤最適化を終了した。平成 26 年度には阪大病院薬剤部で試験薬 GMP リポソーム製造装置を稼働し、平成 27 年度には、早期探索的臨床試験を医師主導型治験として実施する。Lipo-CsA を新規心筋梗塞治療薬としてアカデミア創薬を目指す。

A. 研究目的

　高齢化や糖尿病・脂質代謝異常患者の増加により、急性心筋梗塞発症数は過去 30 年間に3倍に増加している(Takii T, et al. Circ J 2010)。再灌流療法の普及により、急性期死亡率は低下する一方、繰り返す入院が必要な梗塞後心不全患者が著明に増加しており、医療費増大の一因になっている。そのため、慢性期心不全発症を抑制する治療法の開発は重要なアンメットニーズである。梗塞後心不全発症を抑制する方法として、心筋梗塞急性期における薬物補充療法による心筋虚血再灌流障害抑制が期待されるが、未だ確立された治療法はない。近年、動物実験において、サイクロスポリンA(CsA)が虚血再灌流障害を抑制することが報告され、探索的臨床試験においても心筋梗塞サイズの縮小効果が報告された(Piot C et al. N Engl J Med 2008)。しかしながら、CsA の副作用により、臨床投与量に大きな制約がある。

　一方、がんや炎症部位では血管透過性が亢進し、ナノサイズの粒子が血管より流出し、集積する。薬剤をナノリポソームに内包し、炎症部位特異的に薬剤を特異的に送達することにより、薬効の増強と副作用の軽減が期待できる。心筋梗塞部位では激烈な炎症が生じるため、同部位での血管透過性亢進を利用したリポソーム製剤の高い有効性が期待できる。申

請者は研究代表者として、厚生労働科研医療機器開発推進研究事業＜ナノサイズリポソームを用いた急性心筋梗塞治療法の開発＞を実施し、ナノリポソームの心筋梗塞部位へ高い集積による、心保護薬の作用増強と副作用軽減を示した（上図）（Takahama H, et al. J Am Coll Cardiol. 2009; 特願：PCT/JP2008/00652）。本技術を用い、既にラット心筋梗塞モデルにおいて、低用量リポソーム化 CsA の心筋梗塞サイズ縮小増強効果を確認した(特願 2012-117077)。そこで、本研究では、リポソーム化 CsA をアカデミア創薬として開発を進める。

B. 研究成果

(1) 薬効薬理試験

ラット心筋梗塞モデルを用い、再灌流時にリポソーム化サイクロスポリン（Lipo-CsA）、またはサイクロスポリン（CsA）の静脈内単回投与を行った。低用量・高用量いずれの CsA でも心筋梗塞サイズ縮小効果を認めなかったが、低用量 Lipo-CsA で著明な心筋梗塞サイズ縮小効果を認めた。

(2) 薬物動態試験

3H 標識 CsA を封入した Lipo-CsA の体内分布を定量オートラジオグラフィー法で解析し、既知の CsA 体内分布と比較する。リポソーム化による心筋梗塞部位への CsA の集積効果も検討した。

(3) 製剤最適化

GMP リポソーム製剤の組成・製造については、PMDA 薬事戦略相談（対面助言）を反映し、ロット間の均一性を担保しつつ製造する。

また、将来的なコマーシャルベースでの製造を視野に入れた製造装置の最適化検討も行った。

(4) 安全性薬理試験・一般毒性試験

PMDA 薬事戦略相談（対面助言）を反映し、Lipo-CsA を用いた安全性薬理コアバッテリー試験ならびに拡張型単回投与毒性試験を実施中である。

(5) PMDA 相談

前臨床試験ならびに製剤の品質について、薬事戦略相談（対面助言）を実施した（平成 25 年 11 月、平成 26 年 2 月）

C.まとめ

本事業では、心筋梗塞部位を標的とした新規リポソーム製剤の開発により、世界に類をみない独創的な心筋梗塞治療薬の創出が期待され、日本での知的財産蓄積・産業創出に貢献する。さらに、急性心筋梗塞や心不全患者の死亡率低下、また、＜生活の質の低下＞の改善、繰り返す入院の減少により医療費増大抑制に寄与し、アンメットニーズに応えるアカデミア創薬として期待できる。欧米のみならず、経済発展が著しい新興国でも心筋梗塞は激増することが予測される。薬物補充療法による梗塞後心不全抑制療法開発のニーズは極めて大きく、マーケットもグローバルである。

平成 25 年度末までに、薬効薬理試験、薬物動態試験、製剤最適化を終了した。平成 26 年度に、阪大病院薬剤部で GMP リポソーム製造装置を稼働する。平成 25 年以降、安全性薬理試験、毒性試験が開始可能であり、本事業終了時には速やかに医師主導型治験に移行する。心筋梗塞部位での血管透過性亢進に着目し、ナノサイズリポソームを治療に応用するアイディアは画期的であり、PMDA 薬事戦略相談（対面助言）を活用し、特許戦略にも基づいている。

D. 健康危険情報

特記事項なし

E. 研究発表

1. 論文発表

無し

2. 学会発表

無し

F. 知的財産権の出願・登録状況

無し

厚生労働科学研究費補助金（医療技術実用化総合研究事業）
総括研究報告書
急性心筋梗塞治療薬に対する新規治療薬の開発
（H25-医療技術-一般-002）
分担研究者　　中村 歩　大阪大学医学部附属病院薬剤部

研究要旨　急性心筋梗塞発症数は過去20年間に2倍に増加している。繰り返して入院加療が必要な　梗塞後心不全患者が増加しており、国民医療費増大の一因となっている。そのため、梗塞後心不全進展を抑制する治療法の開発は重要なアンメットニーズである。心筋梗塞による細胞死はミトコンドリア Permeability Transition Pore（mPTP）が開口し，チトクロム C の遊離により誘導される。動物実験・探索的臨床試験において、mPTP開口阻害薬であるサイクロスポリンA（CsA）による心筋梗塞サイズ縮小効果が報告されたが、CsA は免疫抑制などの副作用を誘発するため、その臨床投与量に制限がある。申請者は代表研究者として、厚生労働科研医療機器開発推進研究事業＜ナノサイズリポソームを用いた急性心筋梗塞治療法の開発＞で、ナノサイズリポソームが障害心筋へ特異的に集積し、リポソームに封入された心保護薬の薬効増強と副作用軽減を世界に先駆けて見出した。本技術を用い、既に、ラット心筋梗塞モデルにおいて、低用量リポソーム化CsA（Lipo-CsA）による心筋梗塞サイズ縮小増強効果を確認した。さらに、平成25年度末までに、薬効薬理試験、薬物動態試験、製剤最適化を終了した。平成26年度には阪大病院薬剤部で試験薬 GMP リポソーム製造装置を稼働し、平成27年度には、早期探索的臨床試験を医師主導型治験として実施する。Lipo-CsA を新規心筋梗塞治療薬としてアカデミア創薬を目指す。

A. 研究目的

　高齢化や糖尿病・脂質代謝異常患者の増加により、急性心筋梗塞発症数は過去 30 年間に3倍に増加している(Takii T, et al. Circ J 2010)。再灌流療法の普及により、急性期死亡率は低下する一方、繰り返す入院が必要な梗塞後心不全患者が著明に増加しており、医療費増大の一因になっている。そのため、慢性期心不全発症を抑制する治療法の開発は重要なアンメットニーズである。梗塞後心不全発症を抑制する方法として、心筋梗塞急性期における薬物補充療法による心筋虚血再灌流障害抑制が期待されるが、未だ確立された治療法はない。近年、動物実験において、サイクロスポリンA(CsA)が虚血再灌流障害を抑制する

ことが報告され、探索的臨床試験においても心筋梗塞サイズの縮小効果が報告された(Piot C et al. N Engl J Med 2008)。しかしながら、CsA の副作用により、臨床投与量に大きな制約がある。

　一方、がんや炎症部位では血管透過性が亢進し、ナノサイズの粒子が血管より流出し、集積する。薬剤をナノリポソームに内包し、炎症部位特異的に薬剤を特異的に送達することにより、薬効の増強と副作用の軽減が期待できる。心筋梗塞部位では激烈な炎症が生じるため、同部位での血管透過性亢進を利用したリポソーム製剤の高い有効性が期待できる。申請者は研究代表者として、厚生労働科研医療機器開発推進研究事業＜ナノサイズリポソー

ムを用いた急性心筋梗塞治療法の開発＞を
実施し、ナノリポソームの心筋梗塞部位へ高い
集積による、心保護薬の作用増強と副作用軽
減を示した（上図）（Takahama H, et al. J
Am Coll Cardiol. 2009; 特願：
PCT/JP2008/00652）。本技術を用い、既にラ
ット心筋梗塞モデルにおいて、低用量リポソー
ム化 CsA の心筋梗塞サイズ縮小増強効果を
確認した(特願 2012-117077)。そこで、本研究
では、リポソーム化 CsA をアカデミア創薬とし
て開発を進める。

B. 研究成果

(1) 薬効薬理試験

　ラット心筋梗塞モデルを用い、再灌流時にリ
ポソーム化サイクロスポリン（Lipo-CsA）、また
はサイクロスポリン（CsA）の静脈内単回投与を
行った。低用量・高用量いずれの CsA でも心
筋梗塞サイズ縮小効果を認めなかったが、低
用量 Lipo-CsA で著明な心筋梗塞サイズ縮小
効果を認めた。

(2) 薬物動態試験

　3H 標識 CsA を封入した Lipo-CsA の体
内分布を定量オートラジオグラフィー法で解析
し、既知の CsA 体内分布と比較する。リポソー
ム化による心筋梗塞部位への CsA の集積効
果も検討した。

(3) 製剤最適化

　GMP リポソーム製剤の組成・製造について
は、PMDA 薬事戦略相談（対面助言）を反映
し、ロット間の均一性を担保しつつ製造する。

(4) 安全性薬理試験・一般毒性試験

　PMDA 薬事戦略相談（対面助言）を反映し、
Lipo-CsA を用いた安全性薬理コアバッテリー
試験ならびに拡張型単回投与毒性試験を実
施中である。

(5) PMDA 相談

　前臨床試験ならびに製剤の品質について、薬事
戦略相談（対面助言）を実施した（平成 25 年 11 月、
平成 26 年 2 月）

C.まとめ

　本事業では、心筋梗塞部位を標的とした新規
リポソーム製剤の開発により、世界に類をみな
い独創的な心筋梗塞治療薬の創出が期待され、
日本での知的財産蓄積・産業創出に貢献する。
さらに、急性心筋梗塞や心不全患者の死亡率低
下、また、＜生活の質の低下＞の改善、繰り返
す入院の減少により医療費増大抑制に寄与し、
アンメットニーズに応えるアカデミア創薬と
して期待できる。欧米のみならず、経済発展が
著しい新興国でも心筋梗塞は激増することが
予測される。薬物補充療法による梗塞後心不全
抑制療法開発のニーズは極めて大きく、マーケ
ットもグローバルである。

　平成 25 年度末までに、薬効薬理試験、薬物
動態試験、製剤最適化を終了した。平成 26 年
度に、阪大病院薬剤部で GMP リポソーム製造装
置を稼働する。平成 25 年以降、安全性薬理試
験、毒性試験が開始可能であり、本事業終了時
には速やかに医師主導型治験に移行する。心筋
梗塞部位での血管透過性亢進に着目し、ナノサ
イズリポソームを治療に応用するアイディア
は画期的であり、PMDA 薬事戦略相談（対面助言）
を活用し、特許戦略にも基づいている。

D. 健康危険情報

　特記事項なし

E. 研究発表

1. 論文発表

　　　無し

2. 学会発表

　　　無し

F. 知的財産権の出願・登録状況

　　　無し

III. 研究成果の刊行に関する
一覧表

雑誌

発表者氏名	論文タイトル名	発表誌名	巻号	ページ	出版年
Matsuoka K, Asano Y, Higo S, Tsukamoto O, Yan Y, Yamazaki S, Matsuzaki T, Kioka H, Kato H, Uno Y, Asakura M, Asanuma H, Minamino T, Aburatani H, Kitakaze M, Komuro I, Takashima S.	Noninvasive and quantitative live imaging reveals a potential stress-responsive enhancer in the failing heart.	FASEB J	In press	In press	2014
Kioka H, Kato H, Fujikawa M, Tsukamoto O, Suzuki T, Imamura H, Nakano A, Higo S, Yamazaki S, Matsuzaki T, Takafuji K, Asanuma H, Asakura M, Minamino T, Shintani Y, Yoshida M, Noji H, Kitakaze M, Komuro I, Asano Y, Takashima S.	Evaluation of intramitochondrial atp levels identifies g0/g1 switch gene 2 as a positive regulator of oxidative phosphorylation.	Proc Natl Acad Sci USA	111(1)	273-8.	2014
Suna S, Sakata Y, Nakatani D, Okuda K, Shimizu M, Usami M, Matsumoto S, Hara M, Ozaki K, Mizuno H, Minamino T, Takashima S, Nishino M, Matsumura Y, Takeda H, Tanaka T, Sato H, Hori M, Komuro I	Decreased mortality associated with statin treatment in patients with acute myocardial infarction and lymphotoxin-alpha C804A polymorphism.	Atherosclerosis	227(2)	373-9	2013
Takahama H, Shigematsu H, Asai T, Matsuzaki T, Sanada S, Fu HY, Okuda K, Yamato M, Asanuma H, Asano Y, Asakura M, Oku N, Komuro I, Kitakaze M, Minamino T	Liposomal amiodarone augments anti-arrhythmic effects and reduces hemodynamic adverse effects in an ischemia/reperfusion rat model.	Cardiovasc Drugs Ther	27(2)	125-32	2013

Ishii T, Sasai T, Oyama D, Agato Y, Yasuda N, Fukuta T, Shimizu K, Minamino T, Oku N.	Treatment of cerebral ischemia-reperfusion injury with PEGylated liposomes encapsulating FK506	FASEB J	27(4)	1362-70	2013
Takahashi A, Asakura M, Ito S, Min KD, Shindo K, Yan Y, Liao Y, Yamazaki S, Sanada S, Asano Y, Ishibashi-Ueda H, Takashima S, Minamino T, Asanuma H, Mochizuki N, Kitakaza M.	Dipeptidyl-Peptidase IV Inhibition Improves Pathophysiology of Heart Failure and Increases Survival Rate in Pressure-Overloaded Mice.	Am J Physiol Heart Circ Physiol.	304	H1361-9	2013

Ⅳ．研究成果の刊行物・別刷

The FASEB Journal • Research Communication

Noninvasive and quantitative live imaging reveals a potential stress-responsive enhancer in the failing heart

Ken Matsuoka,*,† Yoshihiro Asano,*,†,1 Shuichiro Higo,*,† Osamu Tsukamoto,† Yi Yan,† Satoru Yamazaki,§ Takashi Matsuzaki,* Hidetaka Kioka,*,† Hisakazu Kato,† Yoshihiro Uno,‡ Masanori Asakura,|| Hiroshi Asanuma,¶ Tetsuo Minamino,* Hiroyuki Aburatani,# Masafumi Kitakaze,|| Issei Komuro,* and Seiji Takashima*,†

*Department of Cardiovascular Medicine and †Department of Medical Biochemistry and ‡Laboratory of Reproductive Engineering, Institute of Experimental Animal Sciences, Osaka University Graduate School of Medicine, Suita, Japan; §Department of Cell Biology and ||Department of Clinical Research and Development, National Cerebral and Cardiovascular Center Research Institute, Suita, Japan; ¶Department of Cardiovascular Science and Technology, Kyoto Prefectural University School of Medicine, Kyoto, Japan; and #Genome Science Division, Research Center for Advanced Science and Technology, University of Tokyo, Tokyo, Japan

ABSTRACT   Recent advances in genome analysis have enabled the identification of numerous distal enhancers that regulate gene expression in various conditions. However, the enhancers involved in pathological conditions are largely unknown because of the lack of *in vivo* quantitative assessment of enhancer activity in live animals. Here, we established a noninvasive and quantitative live imaging system for monitoring transcriptional activity and identified a novel stress-responsive enhancer of *Nppa* and *Nppb*, the most common markers of heart failure. The enhancer is a 650-bp fragment within 50 kb of the *Nppa* and *Nppb* loci. A chromosome conformation capture (3C) assay revealed that this distal enhancer directly interacts with the 5′-flanking regions of *Nppa* and *Nppb*. To monitor the enhancer activity in a live heart, we established an imaging system using the firefly luciferase reporter. Using this imaging system, we observed that the novel enhancer activated the reporter gene in pressure overload-induced failing hearts (failing hearts: 5.7±1.3-fold; sham-surgery hearts: 1.0±0.2-fold; *P*<0.001, repeated-measures ANOVA). This method will be particularly useful for identifying enhancers that function only during pathological conditions.—Matsuoka, K., Asano, Y., Higo, S., Tsukamoto, O., Yan, Y., Yamazaki, S., Matsuzaki, T., Kioka, H., Kato, H., Uno, Y., Asakura, M., Asanuma, H., Minamino, T., Aburatani, H., Kitakaze, M., Komuro, I., and Takashima, S. Noninvasive and quantitative live imaging reveals a poten-

tial stress-responsive enhancer in the failing heart. *FASEB J.* 28, 000–000 (2014). www.fasebj.org

GENE EXPRESSION IS REGULATED through the integrated action of many *cis*-regulatory elements, including core promoters, proximal promoters, distant enhancers, and insulators (1). Several methods have been used to explore the function of *cis*-regulatory elements during a variety of developmental stages (2, 3). However, the identification of gene regulatory elements with pathophysiological roles has been technically difficult because there are few appropriate models for monitoring transcriptional activity in live animals under pathological conditions.

Here, we focused on the regulatory elements that are responsive to heart failure. The natriuretic peptides, atrial natriuretic peptide (ANP) and brain natriuretic peptide (BNP), encoded by the neighboring genes *Nppa* and *Nppb* are activated in the embryonic heart, down-regulated after birth, and then reactivated during heart failure. Both peptides are well-known biomarkers that are strongly induced during heart failure and represent its severity. Cardiologists frequently use these peptides as natriuretic and vasorelaxant agents to treat various clinical conditions (4–8). Many studies have tried to elucidate the mechanisms of their transcriptional regulation because factors that regulate these

---

natriuretic peptides are potential therapeutic targets for heart disease (9–14).

Mice transgenic for various loci, including the 5′-flanking regions of the natriuretic peptide genes, have been used to identify the regulatory elements required for transcriptional activation either during heart development or in the diseased heart. These studies reported that the 5′-flanking regions of the natriuretic peptide genes regulated their expression during heart development (9, 10, 13); however, the 5′-flanking regions were not responsible for their specific reactivation in the diseased heart (11, 12). A recent study identified the distal enhancer elements regulating the natriuretic peptide genes in the developing heart by examining cardiac-specific transcription factor binding sites; however, these enhancer elements did not respond to heart failure (14). Therefore, the stress-responsive regulatory elements that function during heart failure have not yet been identified and are potentially located outside the 5′-flanking regions.

In this study, we aimed to identify the novel stress-responsive enhancer elements of the *Nppa* and *Nppb* genes in the failing heart. Furthermore, we established a noninvasive and quantitative live imaging assay to monitor the transcriptional activity of candidate enhancers in the failing heart. *In vivo* live imaging of the firefly luciferase reporter in a single mouse enabled us to analyze the sequential changes in enhancer activity during the progression of heart failure. Combined with a fine mapping technique using epigenetic markers, we identified a 650-bp stress-responsive enhancer that was strongly activated by cardiac hypertrophy and heart failure.

MATERIALS AND METHODS

Animals

All procedures were performed according to the U.S. National Institutes of Health (NIH) Guide for the Care and Use of Laboratory Animals (NIH publication no. 85-23, revised 1996) and were approved by the Animal Experiments Committee, Osaka University (approval no. 21-78-10).

Reagents and antibodies

Phenylephrine (PE) was purchased from Sigma-Aldrich (St. Louis, MO, USA). The anti-RNA polymerase II and anti-histone H3 trimethylated at lysine 4 (H3K4me3) antibodies used for chromatin immunoprecipitation sequencing (ChIP-seq) were kind gifts from Dr. H. Kimura (Graduate School of Frontier Biosciences, Osaka University).

Primary culture of neonatal rat cardiomyocytes

Ventricular myocytes obtained from 1- or 2-d-old Wistar rats were prepared and cultured overnight in Dulbecco's modified Eagle's medium (Sigma-Aldrich) containing 10% FBS, as described previously (15).

Comparative genomics

Genome-wide multiple alignments of the genomic sequences containing the *Nppa* and *Nppb* genes were performed using the University of California Santa Cruz (UCSC) Genome Browser (16); 8 vertebrate species were compared, including mouse (mm9, July 2007), rat (m4, Nov. 2004), human (hg18, Mar. 2006), orangutan (ponAbe2, July 2007), dog (canFam2, May 2005), horse (equCab1, Jan. 2007), opossum (monDom4, Jan. 2006), and chicken (galGal3, May 2006). We used vertebrate Multiz alignment of DNA sequences (17) to analyze the homology of DNA sequences among mouse and other species. We used the Placental Mammal Basewise Conservation assessed by PhyloP (18) to assess the degree of mammalian conservation. Next, we identified discrete conserved fragments. The transcribed sequences within the conserved set were filtered out using known genes, spliced ESTs, and mRNA annotations obtained from the UCSC genome browser. Finally, we manually curated the data set to remove any additional false positives by visual examination of the UCSC genomic data. We defined the noncoding conserved regions (CRs) that were homologous at least in the human and mouse genomes and at least 1 kb away from the transcription start sites as the enhancer candidates.

ChIP sequencing on mouse heart tissues

Whole hearts were isolated from 8-wk-old C57BL6 mice, perfused rapidly with cold PBS, flash-frozen in liquid nitrogen, homogenized using a sterile tissue grinder, and cross-linked with 0.3% paraformaldehyde. Subsequently, chromatin isolation, sonication, and immunoprecipitation using an anti-RNA polymerase II antibody and an anti-H3K4me3 antibody were performed. The ChIP DNA and input samples were sheared by sonication, end-repaired, ligated to the sequencing adapters, and amplified. The purified ChIP DNA library samples were sequenced using the Illumina Genome Analyzer II (Illumina, Inc., San Diego, CA, USA). Unfiltered sequence reads were aligned to the mouse reference genome [U.S. National Center for Biotechnology Information (NCBI) build 37, mm9] using Bowtie. RNA polymerase II- and H3K4me3-enriched regions were identified using MACS (19) with the default parameters.

Lentiviral enhancer assay

Eleven CRs were PCR amplified from the mouse BAC clone containing the *Nppa* and *Nppb* loci (clone RP23-128E8; BACPAC Resources Center, Children's Hospital Oakland, Oakland, CA, USA; primers and probes are listed in Supplemental Table S1). The PCR fragments were subcloned into the pCR-Blunt II-TOPO vector (Invitrogen, Carlsbad, CA, USA) and recombined into a lentiviral vector encoding the firefly luciferase reporter (pGreenFire Transcriptional Reporter Lentivector; System Biosciences, Mountain View, CA, USA). The lentiviral particles were produced by transfection of 293T cells with the 3 lentiviral packaging plasmids (*i.e.*, pMDLg/pRRE, pRSV-Rev, and pMD2.VSV.G) using Lipofectamine 2000 (Invitrogen). The supernatant from 293T cells containing the lentiviral particles was collected 48 h after transfection, sterilized using a 0.45-μm cellulose acetate filter, and concentrated by centrifugation (Peg-it Virus Precipitation Solution, System Biosciences).

Rat neonatal cardiomyocytes isolated as described above were plated in 96-well plates. The next day, the medium was replaced with a serum-free medium containing the lentiviral vector, and the cells were incubated for 12 h. Subsequently, the cardiomyocytes were exposed to 100 μM PE for 48 h prior to the luciferase assay.

RNA extraction and quantitative RT-PCR

The total RNA was prepared from rat cardiomyocytes, rat cardiac fibroblasts, murine hearts, and murine brains using the RNA-Bee RNA isolation reagent (Tel-Test, Friendswood, TX, USA) and then converted to cDNA using the high-capacity cDNA reverse transcription kit (Applied Biosystems, Foster City, CA, USA), according to the manufacturer's instructions. The quantitative RT-PCR was performed using the TaqMan technology and the StepOnePlus real-time PCR System (Applied Biosystems). All samples were processed in duplicate. The level of each transcript was quantified according to the threshold cycle (C_t) method using GAPDH as an internal control. Inventoried TaqMan gene expression assays were used: *Nppa*, Rn0056661, Mm01255748; *Nppb*, Rn00580641, Mm01255770; *Gapdh*, rodent GAPDH control reagent.

3C analysis

The whole hearts of the mice were isolated, perfused rapidly with cold PBS, flash-frozen in liquid nitrogen, homogenized using a sterile tissue grinder, and fixed with 1% paraformaldehyde. The cross-linked tissues utilized for 3C experiments were subjected to digestion with *Bam*HI following standard protocols (20, 21). The mouse BAC DNA containing *Nppa* and *Nppb* (clone RP23-128E8) was used as a control. The TaqMan real-time PCR was performed using probes near the restriction sites; the primers and probes are listed in Supplemental Table S2.

Transgenic mouse enhancer assay

The candidate enhancer regions were cloned into a vector encoding the minimal CMV promoter driving the luciferase gene as described above. Transgenic mouse embryos were generated by pronuclear injection into the zygotes of BDF1 mice using standard methods. Because black fur attenuates light transmission, albino mice were generated by crossing the transgenic founders to ICR albino mice.

In vivo bioluminescence imaging

Prior to *in vivo* imaging, the mice were anesthetized using isoflurane, and the black mice were shaved from the neck to the lower torso to allow the optimal visualization of fluorescence without interference from the black fur. A D-luciferin solution was injected intraperitoneally (150 mg/kg i.p.) or intravenously (75 mg/kg i.v.). The mice were imaged using an *in vivo* live imaging system (IVIS Lumina II; Caliper Life Sciences, Waltham, MA, USA). For quantification, the bioluminescence light intensity was measured at the region of interest and expressed in relative light units (RLU/min) using Living Image 4.0 (Caliper Life Sciences). To calculate the enhancer activity in the heart, we defined the ratio of heart to brain luciferase intensities as the cardiac-specific enhancer activity.

Transverse aortic constriction (TAC)

Transgenic mice aged 8 wk and weighing 20–25 g were subjected to pressure overload, as described previously (22). Briefly, the chest was entered *via* the second intercostal space at the upper left sternal border. After the arch of the aorta was isolated, a TAC was created using a 7-0 suture tied twice around a 27-gauge needle and the aortic arch, between the innominate and left common carotid arteries. After the

suture was tied, the needle was gently removed, yielding 60–80% constriction of the aorta.

PE-induced hypertrophy

Transgenic mice aged 8 wk and weighing 20–25 g were treated with PE (75 mg/kg/d) using an osmotic minipump (Alzet, Cupertino, CA, USA) to induce cardiac hypertrophy, as previously reported (23, 24).

Statistical analysis

Data are expressed as means ± SE. The 2-tailed Student's *t* test and repeated ANOVA were used to analyze differences between the groups. Values of $P < 0.05$ were considered to represent a significant difference.

RESULTS

Identification of candidate enhancers near the *Nppa-Nppb* locus using comparative genomics and ChIP-seq

To identify potential enhancers, we performed a comparative analysis of the genomic sequences of mouse and divergent species and identified CRs that may function as common regulatory sequences (25–27). We defined CRs that were homologous at least in the human and mouse genomes and at least 1 kb away from the transcription start sites of *Nppa* and *Nppb* as the candidate enhancers. First, we analyzed the 50-kb *Nppa-Nppb* locus bounded by the binding sites of 2 CCCTC-binding factors (CTCFs), which can function as insulators (28, 29). Using a genome database (30), we identified 11 CRs, including the *Nppa* and *Nppb* introns in the 50-kb region (**Fig. 1**).

Next, we performed a ChIP-seq analysis on RNA polymerase II and H3K4me3 in the adult mouse heart. We analyzed the epigenetic modifications near the *Nppa* and *Nppb* genes combined with the ChIP-seq analysis using a public database of the adult mouse heart (30). We hypothesized that the normal heart would have activated epigenetic marks because *Nppa* and *Nppb* are expressed, albeit at low levels, in normal conditions. Recent genome-wide studies have determined that enhancers can be defined as DNA sequences bound by the RNA polymerase II and transcriptional coactivator protein p300, and where histone H3 monomethylated at lysine 4 (H3K4me1) accumulates instead of H3K4me3 (31–34). Among the 11 CRs identified, only CR9 coincided with the binding sites of RNA polymerase II and p300, and overlapped with the gene areas modified by H3K4me1, and filled all criteria for the enhancer (Fig. 1). In addition, H3K4me1 modifications in CR9 were only observed in the heart but not in the other organs (Fig. 1 and Supplemental Fig. S1). Therefore, we analyzed the 11 CRs, including CR9, as the most likely distal candidate enhancers for the stress-responsive regulatory regions of the natriuretic peptide genes.
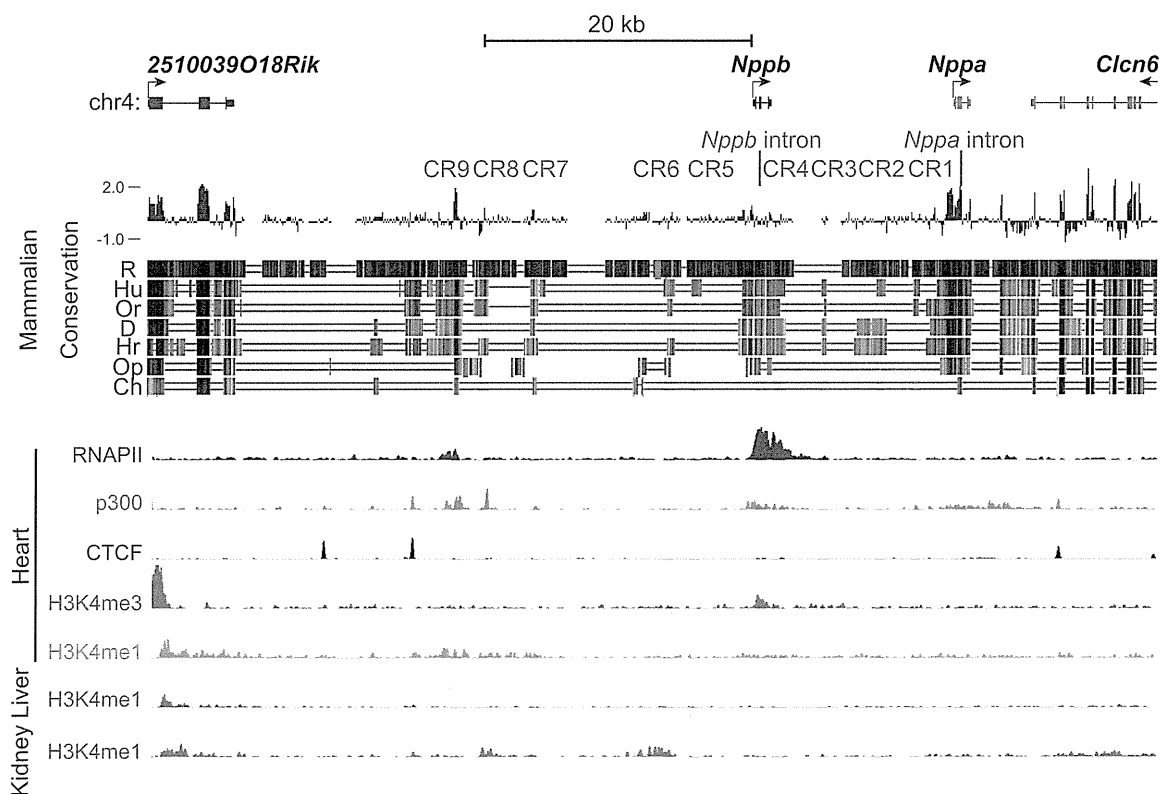
Figure 1. Mammalian evolutionarily conserved regions and ChIP-seq data surrounding the murine *Nppa* and *Nppb* loci. We used an open database on the University of California Santa Cruz (UCSC) Genome Browser to assess the degree of DNA sequence conservation around *Nppa* and *Nppb* gene loci. Blue and red vertical lines, the Placental Mammal Basewise Conservation assessed by PhyloP; black vertical lines, the vertebrate Multiz alignment of DNA sequences among mice and 7 other species (rats, humans, orangutans, dogs, horses, opossums, and chickens). We defined noncoding conserved regions (CRs) that were homologous at least in the human and mouse genomes and at least 1 kb away from the transcription start sites of *Nppa* and *Nppb* as the candidate enhancers. CRs are highlighted as light red vertical bars (CR1-9, *Nppa* intron, and *Nppb* intron). ChIP-seq data for H3K4me1, p300, and CTCF were obtained from an open database of the adult mouse heart. Some CRs coincided with the peaks for H3K4me1, RNA polymerase II, and the transcriptional coactivator protein p300. R, rat; Hu, human; Or, orangutan; D, dog; Hr, horse; Op, opossum; Ch, chicken.

Identification of a distal enhancer element responsive to an α₁-adrenergic receptor agonist

We screened the candidate enhancers for potential stress-responsive regulatory regions. We analyzed the enhancer activity of these 11 CRs after treatment with PE, an α_1-adrenergic receptor agonist, which mimics cardiac overload and induces *Nppa* and *Nppb* expression in cardiomyocytes (35). We confirmed that PE induced the expression of endogenous *Nppa* and *Nppb* specifically in cardiomyocytes but not in cardiac fibroblasts (**Fig. 2A**). Then, we introduced the 11 CRs with a minimum human cytomegalovirus (CMV) promoter and the luciferase gene into rat cardiomyocytes using a lentiviral vector system.

Among the 11 CRs tested, only CR9, which is located 22 kb upstream from the *Nppb* transcription start site and shows high mammalian conservation score in the Placental Mammal Basewise Conservation by PhyloP (Fig. 2*B*), reproducibly increased the PE-induced luciferase activity by ~5-fold compared to the minimal CMV promoter alone (Fig. 2*C*). However, CR9 did not respond to PE in cardiac fibroblasts (Fig. 2*C*). These

results suggest that CR9 is the regulatory element that is responsive to PE specifically in cardiomyocytes.

Long-range physical interaction between the distal enhancer element and the proximal promoters of the *Nppa* and *Nppb* genes

Confirming the looping interactions between distal elements and promoters is one way to demonstrate the transcriptional regulatory activity of distal elements. We performed a 3C assay (20) to comprehensively investigate whether the genomic region containing CR9 moved closer to the *Nppa* or *Nppb* promoter in an adult murine heart treated with a continuous infusion of PE *in vivo*.

The ligation frequencies were quantified by TaqMan real-time PCR using specific primers and probes and were compared to the ligation frequency of noncross-linked *Bam*HI-digested BAC DNA containing the *Nppa-Nppb* locus. We observed that CR9 interacts with both the *Nppa* and *Nppb* promoter regions at a higher frequency relative to other gene areas (Fig. 2*D*); furthermore, PE treatment strengthened these interac-
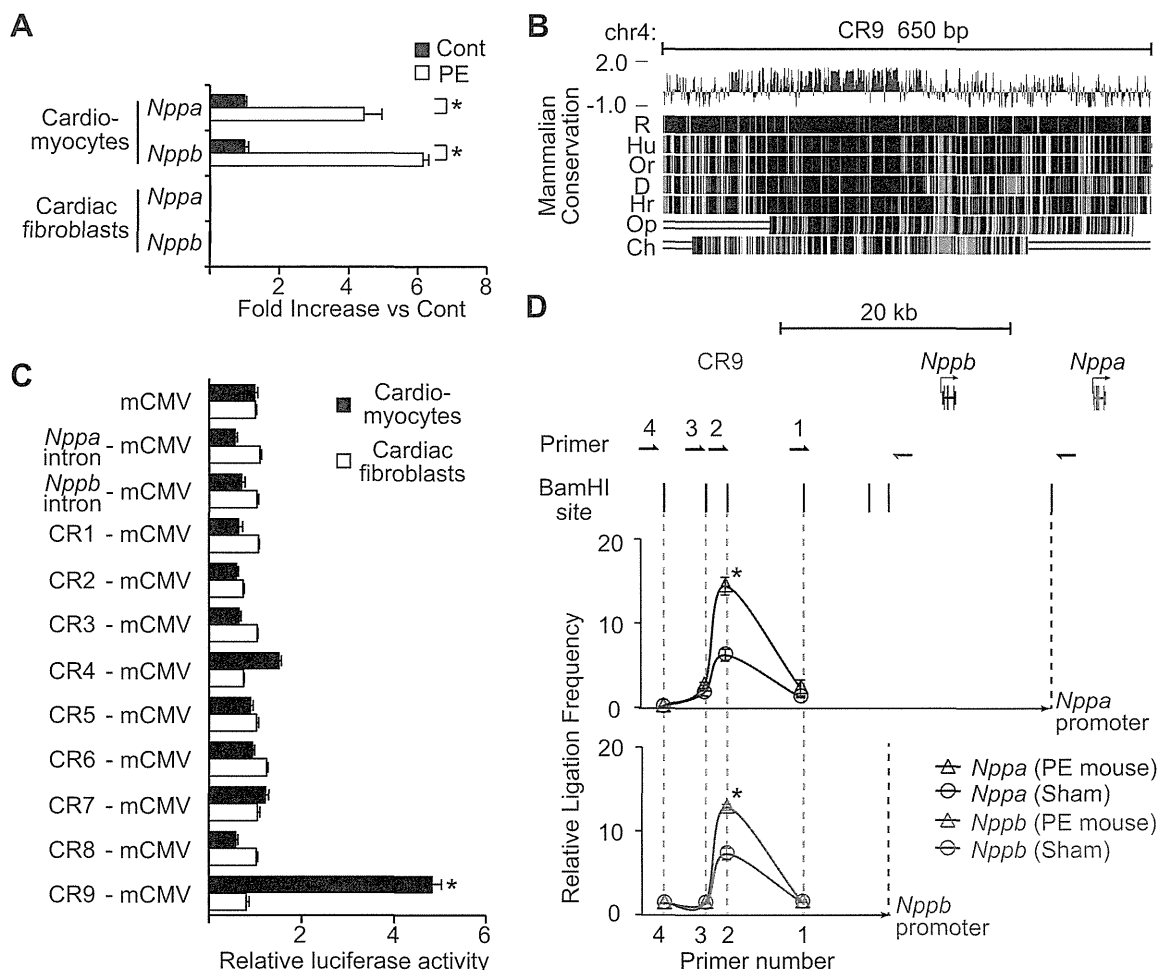
Figure 2. Identification of a distal enhancer element that is responsive to an α_1-adrenergic receptor agonist. *A*) Relative transcript levels of *Nppa* and *Nppb* in rat neonatal cardiomyocytes and cardiac fibroblasts 48 h after treatment with PE (100 μM). Values are means ± se (*n*=3 cultures). *P < 0.01 vs. control; *t* test. *B*) CR9 is a highly conserved genomic region in vertebrates. *C*) Relative luciferase reporter activities of CRs in rat neonatal cardiomyocytes and cardiac fibroblasts 48 h after treatment with PE (100 μM). PE-induced luciferase activity driven by the mCMV promoter was defined as 1. Values are means ± se (*n*=5 cultures). *P < 0.001 vs. mCMV alone; *t* test. *D*) In vivo 3C analysis of the murine *Nppa* and *Nppb* loci, showing relative ligation frequencies of each primer to the *Nppa* promoter (blue triangle, mouse with PE treatment; blue circle, mouse without PE) and the *Nppb* promoter (red triangle, mouse with PE treatment; red circle, mouse without PE). Vertical bars and arrows show the positions of *Bam*HI sites and primers. Data were normalized to the amplification value of a *Bam*HI-digested and religated BAC clone, which included the *Nppa* and *Nppb* loci (means ± se; *n*=2 hearts). R, rat; Hu, human; Or, orangutan; D, dog; Hr, horse; Op, opossum; Ch, chicken. *P < 0.05 vs. control; *t* test.

tions (Fig. 2*D*). These results suggest that there is a close proximity between the distal genomic region containing CR9 and the proximal promoters of the *Nppa* and *Nppb* genes in the PE-induced hypertrophic heart.

Establishment of an *in vivo* live imaging system for gene expression in a murine model of heart disease

We confirmed the activity of the newly identified enhancer CR9 in the heart *in vivo*. The conventional histological evaluation of LacZ reporter expression in the heart only provides data at a single time point; therefore, this method cannot be employed for kinetic assessments or time course analyses of reporter expression in a live heart.

To overcome this difficulty, we established a nonin-

vasive and quantitative live imaging system that allowed real-time monitoring of the firefly luciferase reporter. We generated 3 transgenic mouse lines (Tg-line1, Tg-line2, and Tg-line3) in which the CR9 enhancer element and a minimal CMV promoter driving the luciferase reporter gene were introduced into the germline. The live-imaging system detected luciferase expression in the heart, brain, and intestine of the Tg-line1 (**Fig. 3***A*), in the heart, salivary glands, and skin of the Tg-line2 (Supplemental Fig. S2*A*), and in the heart of the Tg-line3 (Supplemental Fig. S2*E*).

To identify the organs in which CR9 functioned as a stress-responsive enhancer, we examined the luciferase reporter expression in each organ by quantitative PCR. Continuous infusion of PE increased the blood pressure and resulted in cardiac hypertrophy (24, 36). The
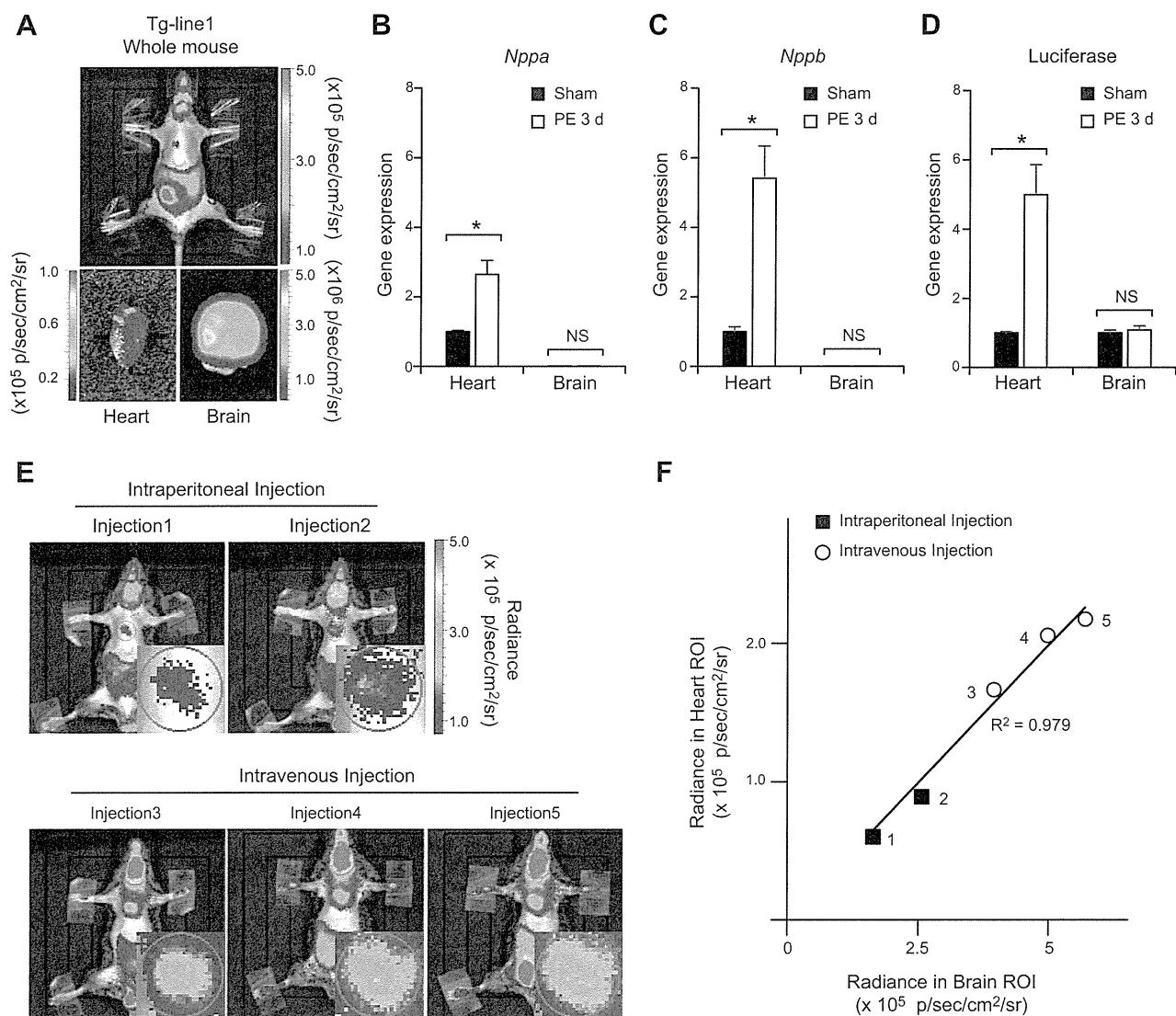
Figure 3. Establishment of an *in vivo* live imaging system for enhancer activity. *A*) Chemiluminescence imaging of CR9 in a mouse of Tg-line1. Top panel: result from whole-animal *in vivo* live imaging. Bottom panels: chemiluminescence images of the heart and brain in the same mouse. *B, C*) Relative transcript levels of *Nppa* and *Nppb* in the ventricular myocardium and brain of CR9 Tg-line1 mice treated with continuous infusion of PE for 3 d. Average transcript level in the ventricular myocardium of preinfused mice was defined as 1 (means ± SE; n=5 hearts). *$P < 0.01$ *vs.* sham-infused mice; t test. *D*) Relative transcript levels of luciferase reporter in the ventricular myocardium and brain of the CR9 Tg-line1 mice continuously infused with PE for 3 d. Average transcript level in the ventricular myocardium and brain of preinfused mice was defined as 1. (means ± SE; n=5 hearts). *$P < 0.01$ *vs.* sham-infused mice; t test. *E*) Comparison of the chemiluminescence intensities obtained using different luciferin injection methods in a Tg-line1 mouse; injections 1 and 2, intraperitoneal injections (top panels), injections 3, 4, and 5, intravenous injections (bottom panels). Injections were performed ≥4 h apart to eliminate the effect of the previous injection. Inset in each panel shows a magnified image of the heart. *F*) Scatterplots of the chemiluminescence intensities in the heart and brain. Plots indicate the independent experiments shown in each panel in *E*. There is a linear relationship between the expression in the heart and the brain, R^2 = 0.979.

expression of endogenous *Nppa* and *Nppb* mRNA increased 3 d after the PE infusion began (Fig. 3*B*, *C* and Supplemental Fig. S2*B*, *C*, *F*, *G*). Concomitantly, the quantitative PCR analysis of the CR9 luciferase mRNA expression showed enhanced expression in the ventricular myocardium 3 d after the PE infusion (Fig. 3*D* and Supplemental Fig. S2*D*, *H*). On the other hand, in the brain and the salivary glands where neither *Nppa* nor *Nppb* is highly expressed, the CR9-driven luciferase mRNA expression did not respond to PE (Fig. 3*B*–*D* and Supplemental Fig. S2*B*–*D*, *F*–*H*). Therefore, the

patterns of PE-induced luciferase expression suggest that CR9 is almost exclusively active in the heart. Because the integration sites were random in these three lines, the patterns of luciferase expression depend on CR9 or other enhancers near the integrated sites. The expression of luciferase in the brain of Tg-line1 and salivary glands of Tg-line2, both of which express neither *Nppa* nor *Nppb*, might be driven by other enhancers near the integrated sites.

To evaluate the accuracy and reproducibility of this method, we measured the luminescence in the heart of

a mouse from Tg-line1. In this transgenic line, the brain, intestine, and testis expressed the reporter protein due to positional effects of the insertion site and most likely not due to CR9 activity. Because the luciferase mRNA expression in the brain remained unchanged after PE treatment (Fig. 3D), we used the reporter activity in the brain as a control. The absolute luminescence values of the heart were affected by the injection method and the amount of luciferase substrate injected (Fig. 3E). However, using brain luminescence as a control, we successfully eliminated the signal variations caused by these differences. The ratio of the luminescence in the heart and brain remained constant within each mouse, independent of the injection method (Fig. 3F). Therefore, we defined the ratio of heart to brain luciferase intensities as the cardiac-specific enhancer activity.

Distal enhancer element was activated in the murine model of heart failure

To examine whether the CR9 enhancer was also responsible for gene expression in other pathological conditions, we subjected Tg-line1 mice to heart failure induced by TAC and compared them with sham-surgery mice. This model mimics the heart condition of patients with hypertension who suffer a continuous pressure overload on the heart. The pressure overload by TAC caused potent cardiac hypertrophy at 2 wk postsurgery and reduced cardiac contractility at 3 wk postsurgery (**Fig. 4A, B**), as previously reported (22). The endogenous *Nppa* and *Nppb* expression increased severalfold in the ventricular myocardium 3 wk after the TAC surgery (Fig. 4C). The heart to brain luciferase intensity ratio also increased severalfold 3 wk following the TAC surgery (Fig. 4D, E and Supplemental Fig. S3). However, the heart to brain luciferase intensity ratio of sham-surgery mice did not change after the surgery (Fig. 4D, E and Supplemental Fig. S3; 3 wk after TAC surgery: 5.7 ± 1.3 fold; 3 wk after sham surgery: 1.0 ± 0.2 fold; $P < 0.001$, repeated ANOVA). These results suggest that CR9 increases transcriptional activity during mechanical pressure overload-induced hypertrophy and subsequent heart failure.

DISCUSSION

Here, we focused on the stress-responsive regulatory elements of *Nppa* and *Nppb* in heart failure. By screening the evolutionarily conserved and epigenetically modified regions around the *Nppa* and *Nppb* gene loci, we identified a 650-bp transcriptional enhancer that was responsive to an α_1-adrenergic receptor agonist *in vitro*. Furthermore, *in vivo* 3C analysis revealed that this distal enhancer directly interacted with the 5′-flanking regions of both *Nppa* and *Nppb*. Using *in vivo* live imaging of luciferase reporter gene expression, we observed that this 650-bp enhancer caused cardiac-specific activation of reporter gene expression during

the progression of pressure overload-induced heart failure. Notably, this is the first study to provide a time series analysis for monitoring enhancer activity under pathological conditions in an individual live mouse.

Although numerous approaches have been used to explore the stress-responsive regulatory elements driving gene transcription during heart failure (11, 12, 14), these elements have not yet been identified due to the technical difficulty involved. To detect the elements that are responsive to pathological conditions such as heart failure, it is essential to confirm the activity of the responsive element using a beating heart that remains connected to the systemic cardiovascular system. Therefore, it would be beneficial to establish transgenic mouse lines carrying a reporter plasmid to assess the responsive elements driving the expression of specific genes. However, the creation of multiple stable adult mouse lines to identify these elements is time-consuming.

In this study, we utilized two improved methods for reporter analysis and successfully identified a novel potent enhancer.

First, by performing an enhancer analysis using a lentiviral vector, we accurately identified candidate enhancers in cardiomyocytes and subsequently generated transgenic reporter mice. Previous promoter analyses used electroporation or lipofection to transfect cultured cardiomyocytes with plasmids (37, 38), but the transfection efficiency of these methods in primary cardiomyocytes is too low to accurately measure reporter activity during the stress response. In this study, greater than 90% transduction efficiency of cardiomyocytes was achieved using a lentiviral vector, which enabled us to accurately identify a specific enhancer fragment. Using this method, we efficiently minimized the number of reporter plasmids to be subsequently integrated into the mouse genome to screen for potential enhancers.

Second, by sequentially measuring the enhancer activity in a single live mouse, we collected robust data to assess enhancer activity in the heart *in vivo*. LacZ is not a suitable reporter for this purpose because LacZ activity can only be assessed after animal euthanization. Therefore, we overcame this limitation using the luciferase reporter plasmid. Recent advances in high-sensitivity luminescence imaging have made it possible to evaluate enhancer-driven luciferase activity without operating on the mice. Therefore, we sequentially assessed reporter activity and hemodynamic changes in the same mouse throughout the time course of the development of heart failure. These data were highly reproducible and enabled us to identify an enhancer element that was activated by cardiac overload. Because this method can be applied to any organ, the *in vivo* luciferase reporter assay may be used for assessing the *in vivo* enhancer or promoter activities responsible for clinically important diseases. The noninvasive nature of this method also enabled us to simultaneously assess the hemodynamic and metabolic parameters *in vivo* along with reporter activity. Specifically, the Tg-line1
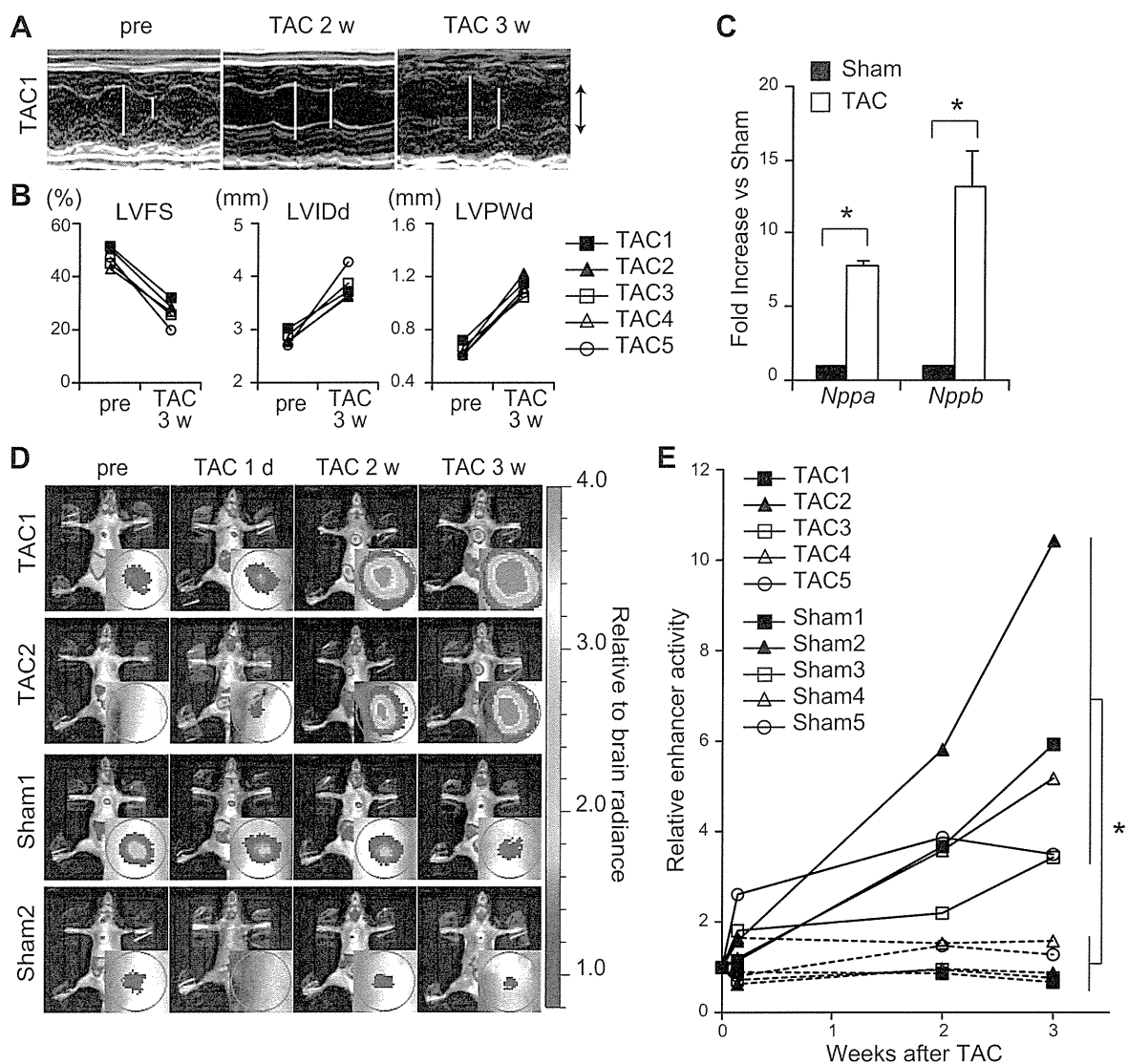
Figure 4. Distal enhancer element is reactivated in the murine model of heart failure. *A*) Representative M-mode echocardiograms in a mouse of Tg-line1 (TAC1) before and after TAC. Open bars indicate maximal left ventricular internal dimension in diastole (LVIDd) and maximal left ventricular internal dimension in systole (LVIDs). Up and down arrows represent 3 mm. *B*) Echocardiographic changes in left ventricular fractional shortening (LVFS), LVIDd, and left ventricular posterior wall thickness in diastole (LVPWd) in 5 mice of Tg-line1 (TAC1-5) before and after TAC. *C*) Relative *Nppa* and *Nppb* transcript levels in the ventricular myocardium 3 wk after the TAC procedure (means ± SE; *n*=3 hearts). *$P < 0.05$ *vs.* sham-surgery mice; *t* test. *D*) Sequential *in vivo* live imaging of 4 representative Tg-line1 mice before and after TAC or sham surgery at each time point. Top 2 and bottom 2 panels represent sequential imaging data of TAC and sham-surgery mice, respectively. Sequential imaging of the 6 other surgically treated mice is shown in Supplemental Fig. S3. Insets in images show magnified images of the heart. Color scale depends on the ratio relative to brain intensity. *E*) Cardiac-specific enhancer activity plots of 10 Tg-line1 mice (TAC1, TAC2, and Sham1, Sham2, shown in *D*) and TAC3–5 and Sham3–5 shown in Supplemental Fig. S3). Heart to brain luciferase intensity ratio represents the cardiac-specific enhancer activity; enhancer activity in presurgery mice was defined as 1. 3 wk after TAC surgery: 5.7 ± 1.3 fold; 3 wk after sham surgery: 1.0 ± 0.2 fold; means ± SE; *n* = 5. *$P < 0.001$, repeated ANOVA.

mice enabled us to accurately quantify the expression level of the natriuretic peptides. These mice are useful tools for repeatedly assessing the degree of heart failure to screen various cardiovascular drugs.

The integration of activities from multiple enhancers could confer specificity and robustness to transcriptional regulation (1). Warren *et al.* (14) identified the *Nppa* enhancer in the embryonic heart by examining Nkx2-5 binding regions around the *Nppa* locus, but the

enhancer did not respond to heart failure. This enhancer does not overlap with CR9 and might regulate *Nppa* expression only during the embryonic stage (14). On the other hand, Horsthuis *et al.* (11) showed that the regulatory region from −27 to +58 kb relative to the transcription start site of *Nppa* was sufficient for *Nppa* gene expression in the failing heart, similar to CR9. However, because this 85-kb regulatory region does not include CR9, *Nppa* may have multiple enhanc-

ers that regulate its expression during heart failure. Furthermore, the length of the 85-kb region poses a challenge for understanding its specific biological role.

This is the first study to provide a time course imaging analysis of enhancer activity using an individual live diseased mouse model. Using this new method, we identified a novel heart enhancer. This method can be widely used for identifying enhancers that regulate transcriptional activity only under pathological conditions. □FJ

REFERENCES

1. Spitz, F., and Furlong, E. E. (2012) Transcription factors: from enhancer binding to developmental control. *Nat. Rev. Genet.* **13**, 613–626
2. Chien, K. R., Domian, I. J., and Parker, K. K. (2008) Cardiogenesis and the complex biology of regenerative cardiovascular medicine. *Science* **322**, 1494–1497
3. Olson, E. N. (2006) Gene regulatory networks in the evolution and development of the heart. *Science* **313**, 1922–1927
4. Burley, D. S., and Baxter, G. F. (2007) B-type natriuretic peptide at early reperfusion limits infarct size in the rat isolated heart. *Basic Res. Cardiol.* **102**, 529–541
5. Holtwick, R., van Eickels, M., Skryabin, B. V., Baba, H. A., Bubikat, A., Begrow, F., Schneider, M. D., Garbers, D. L., and Kuhn, M. (2003) Pressure-independent cardiac hypertrophy in mice with cardiomyocyte-restricted inactivation of the atrial natriuretic peptide receptor guanylyl cyclase-A. *J. Clin. Invest.* **111**, 1399–1407
6. Kitaze, M., Asakura, M., Kim, J., Shintani, Y., Asanuma, H., Hamasaki, T., Seguchi, O., Myoishi, M., Minamino, T., Ohara, T., Nagai, Y., Nanto, S., Watanabe, K., Fukuzawa, S., Hirayama, A., Nakamura, N., Kimura, K., Fujii, K., Ishihara, M., Saito, Y., Tomoike, H., and Kitamura, S. (2007) Human atrial natriuretic peptide and nicorandil as adjuncts to reperfusion treatment for acute myocardial infarction (J-WIND): two randomised trials. *Lancet* **370**, 1483–1493
7. Li, P., Wang, D., Lucas, J., Oparil, S., Xing, D., Cao, X., Novak, L., Renfrow, M. B., and Chen, Y. F. (2008) Atrial natriuretic peptide inhibits transforming growth factor beta-induced Smad signaling and myofibroblast transformation in mouse cardiac fibroblasts. *Circ. Res.* **102**, 185–192
8. Tamura, N., Ogawa, Y., Chusho, H., Nakamura, K., Nakao, K., Suda, M., Kasahara, M., Hashimoto, R., Katsuura, G., Mukoyama, M., Itoh, H., Saito, Y., Tanaka, I., Otani, H., and Katsuki, M. (2000) Cardiac fibrosis in mice lacking brain natriuretic peptide. *Proc. Natl. Acad. Sci. U. S. A.* **97**, 4239–4244
9. De Lange, F. J., Moorman, A. F., and Christoffels, V. M. (2003) Atrial cardiomyocyte-specific expression of Cre recombinase driven by an Nppa gene fragment. *Genesis* **37**, 1–4
10. Habets, P. E., Moorman, A. F., Clout, D. E., van Roon, M. A., Lingbeek, M., van Lohuizen, M., Campione, M., and Christoffels, V. M. (2002) Cooperative action of Tbx2 and Nkx2.5 inhibits ANF expression in the atrioventricular canal: implications for cardiac chamber formation. *Genes Dev.* **16**, 1234–1246
11. Horsthuis, T., Houweling, A. C., Habets, P. E., de Lange, F. J., el Azzouzi, H., Clout, D. E., Moorman, A. F., and Christoffels, V. M. (2008) Distinct regulation of developmental and heart disease-induced atrial natriuretic factor expression by two separate distal sequences. *Circ. Res.* **102**, 849–859
12. Knowlton, K. U., Rockman, H. A., Itani, M., Vovan, A., Seidman, C. E., and Chien, K. R. (1995) Divergent pathways mediate the induction of ANF transgenes in neonatal and hypertrophic ventricular myocardium. *J. Clin. Invest.* **96**, 1311–1318
13. Small, E. M., and Krieg, P. A. (2003) Transgenic analysis of the atrialnatriuretic factor (ANF) promoter: Nkx2-5 and GATA-4 binding sites are required for atrial specific expression of ANF. *Dev. Biol.* **261**, 116–131
14. Warren, S. A., Terada, R., Briggs, L. E., Cole-Jeffrey, C. T., Chien, W. M., Seki, T., Weinberg, E. O., Yang, T. P., Chin, M. T., Bungert, J., and Kasahara, H. (2011) Differential role of Nkx2-5 in activation of the atrial natriuretic factor gene in the developing versus failing heart. *Mol. Cell. Biol.* **31**, 4633–4645
15. Simpson, P., McGrath, A., and Savion, S. (1982) Myocyte hypertrophy in neonatal rat heart cultures and its regulation by serum and by catecholamines. *Circ. Res.* **51**, 787–801
16. Siepel, A., Bejerano, G., Pedersen, J. S., Hinrichs, A. S., Hou, M., Rosenbloom, K., Clawson, H., Spieth, J., Hillier, L. W., Richards, S., Weinstock, G. M., Wilson, R. K., Gibbs, R. A., Kent, W. J., Miller, W., and Haussler, D. (2005) Evolutionarily conserved elements in vertebrate, insect, worm, and yeast genomes. *Genome Res.* **15**, 1034–1050
17. Blanchette, M., Kent, W. J., Riemer, C., Elnitski, L., Smit, A. F., Roskin, K. M., Baertsch, R., Rosenbloom, K., Clawson, H., Green, E. D., Haussler, D., and Miller, W. (2004) Aligning multiple genomic sequences with the threaded blockset aligner. *Genome Res.* **14**, 708–715
18. Pollard, K. S., Hubisz, M. J., Rosenbloom, K. R., and Siepel, A. (2010) Detection of nonneutral substitution rates on mammalian phylogenies. *Genome Res.* **20**, 110–121
19. Zhang, Y., Liu, T., Meyer, C. A., Eeckhoute, J., Johnson, D. S., Bernstein, B. E., Nusbaum, C., Myers, R. M., Brown, M., Li, W., and Liu, X. S. (2008) Model-based analysis of ChIP-Seq (MACS). *Genome Biol.* **9**, R137
20. Dekker, J., Rippe, K., Dekker, M., and Kleckner, N. (2002) Capturing chromosome conformation. *Science* **295**, 1306–1311
21. Hagege, H., Klous, P., Braem, C., Splinter, E., Dekker, J., Cathala, G., de Laat, W., and Forne, T. (2007) Quantitative analysis of chromosome conformation capture assays (3C-qPCR). *Nat. Protoc.* **2**, 1722–1733
22. Liao, Y., Ishikura, F., Beppu, S., Asakura, M., Takashima, S., Asanuma, H., Sanada, S., Kim, J., Ogita, H., Kuzuya, T., Node, K., Kitakaze, M., and Hori, M. (2002) Echocardiographic assessment of LV hypertrophy and function in aortic-banded mice: necropsy validation. *Am. J. Physiol. Heart Circ. Physiol.* **282**, H1703–H1708
23. Saadane, N., Alpert, L., and Chalifour, L. E. (1999) Expression of immediate early genes, GATA-4, and Nkx-2.5 in adrenergic-induced cardiac hypertrophy and during regression in adult mice. *Brit. J. Pharmacol.* **127**, 1165–1176
24. Vecchione, C., Fratta, L., Rizzoni, D., Notte, A., Poulet, R., Porteri, E., Frati, G., Guelfi, D., Trimarco, V., Mulvany, M. J., Agabiti-Rosei, E., Trimarco, B., Cotecchia, S., and Lembo, G. (2002) Cardiovascular influences of α1β-adrenergic receptor defect in mice. *Circulation* **105**, 1700–1707
25. Nobrega, M. A., Ovcharenko, I., Afzal, V., and Rubin, E. M. (2003) Scanning human gene deserts for long-range enhancers. *Science* **302**, 413
26. Thomas, J. W., Touchman, J. W., Blakesley, R. W., Bouffard, G. G., Beckstrom-Sternberg, S. M., Margulies, E. H., Blanchette, M., Siepel, A. C., Thomas, P. J., McDowell, J. C., Maskeri, B., Hansen, N. F., Schwartz, M. S., Weber, R. J., Kent, W. J.,